Journal of Sound and Vibration (2002) **254**(3), 523–539
doi:10.1006/jsvi.2001.4107, available online at http://www.idealibrary.com on IDEAL®

RESPONSE OF A PLATE TO DIFFUSE ACOUSTIC FIELD USING STATISTICAL ENERGY ANALYSIS

K. Renji and P. S. Nair

Structures Group, ISRO Satellite Centre, Bangalore 560017, *India. E-mail: renji@isac.ernet.in*

and

S. Narayanan

Department of Applied Mechanics, Indian Institute of Technology, Chennai 600 036, *India*

(*Received* 31 *October* 2000, *and in final form* 29 *May* 2001)

Inclusion of non-resonant component is expected to improve the estimation of response of a structure to acoustic excitation. In this paper this is verified experimentally. A typical plate is subjected to acoustic excitation in a reverberant chamber and the acceleration responses are measured. The experimental results match well with the theoretical estimates that are made incorporating the non-resonant component. The results show that if the non-resonant part is not considered, the estimated response is in large error. This is seen in the spatial average response as well as in the response levels for a confidence coefficient of 99%.

1. INTRODUCTION

Statistical energy analysis (SEA) developed by Lyon [1] and others is the widely used technique in estimating the response of multi-modal systems at high frequencies. The "high frequency" here means the frequency at which the acoustical/structural wavelength is smaller than the dimensions of the structure. In SEA, the entire system is considered to be an assembly of a number of structural elements, called subsystems. In many cases, the subsystems can be physically identifiable structural parts. Reverberant acoustic field itself it represented as one subsystem in the SEA formulation. Power balance of these subsystems forms the basis for SEA calculations.

In SEA, responses are averaged over a frequency band having several modes and not obtained at a particular frequency. Responses at different locations are treated as an ensemble of random processes and hence statistical quantities like mean (spatial), variance, etc., are determined. Also, the response predicted by SEA is the average over an ensemble of systems.

The response of a structure to acoustic excitation can be split into two components [2–4]. One component is the resonant part which is due to the structural modes. The resonant response depends primarily on the acoustic radiation resistance of the structure. The second component is the non-resonant response that is due to the trace wave generated in the structure by the acoustic field.

Expressions for the frequency averaged radiation resistance of plates into a reverberant room were originally derived by Maidanik [5]. These expressions with certain modifications are generally used in estimating the radiation resistance of plates [6, 7]. Renji

0022-460X/02/$35.00

et al. [8] showed that the above expressions overestimate the radiation resistance. They derived an expression for the radiation resistance which gives half the radiation resistance of what is given by the existing expressions up to the critical frequency of the plate. These findings were validated by the experimental results [8].

Conventional SEA modelling does not predict the non-resonant response of the structure [9]. But the non-resonant response can be as significant as resonant response, especially in the case of structural panels, at frequencies near and above the critical frequency. Renji *et al.* [9] derived an expression for the non-resonant response of a plate due to the diffuse field and they also developed an alternate SEA modelling technique that predicts the non-resonant response of the structure.

The inclusion of the non-resonant component in the response prediction and the modification of the expression for the radiation resistance are expected to improve the estimation of the response of plates to diffuse acoustic field using SEA. The present study aims at verifying this. Hence, the response of a plate when subjected to reverberant acoustic excitation is obtained experimentally. They are compared with the response of the same plate estimated using SEA with the modified expression for the radiation resistance and incorporating the non-resonant component. The significance of the non-resonant response is clear when the experimental results are compared with the theoretical estimates made without considering the non-resonant part. It is to be noted that the improvements made in the estimation of radiation resistance by the use of modified expression for the radiation resistance is clear from the measured radiation resistance of the plate [8] and hence it is not attempted here.

2. EXPERIMENTAL RESULTS

A typical plate is subjected to acoustic excitation in a reverberant chamber and the responses are measured. The plate is suspended in the reverberant chamber and the acoustic field is generated using electro-pneumatic transducers and horns. The boundaries of the plate are free. The test set-up is shown in Figure 1.

The reverberation chamber has dimensions of $10{\cdot}33 \times 8{\cdot}2 \times 13{\cdot}0$ m. The medium of the chamber is air. The temperature of the air during the test was 25°C and the relative humidity was 51%. For these conditions the density of the air is taken as $1{\cdot}21$ kg/m^3 and the speed of sound in air is 346 m/s. The frequency of the first acoustic mode in the chamber is 13·3 Hz. In the third octave bands centered at 63 Hz and above, the SPL in the chamber is almost uniform. In the third octave band centered at 63 Hz, there are 19 modes in the chamber.

The plate is made of aluminum having the dimensions of $2{\cdot}19 \times 1{\cdot}22$ m and thickness 4·95 mm. Young's modulus of the material is $7{\cdot}2 \times 10^{10}$ N/m^2, the Poisson ratio is 0·3 and the density is 2800 kg/m^3. The modal density $n(f)$ of the plate at frequency f is calculated as 0·176 Hz using the equation

$$n(f) = (A/2)\,(\rho/D)^{1/2}, \tag{1}$$

where A is the area, ρ is the mass per unit area and D is the flexural rigidity of the plate. The critical frequency, denoted by f_c is calculated at 2512 Hz using equation (1)

$$f_c^2 = (c^4\rho/D)/(4\pi^2), \tag{2}$$

where c is the speed of sound in the acoustic medium of the chamber.

The sound pressure levels (SPL) in the room are measured using condenser-type microphones at three locations and the spatial average is taken as the excitation SPL. The

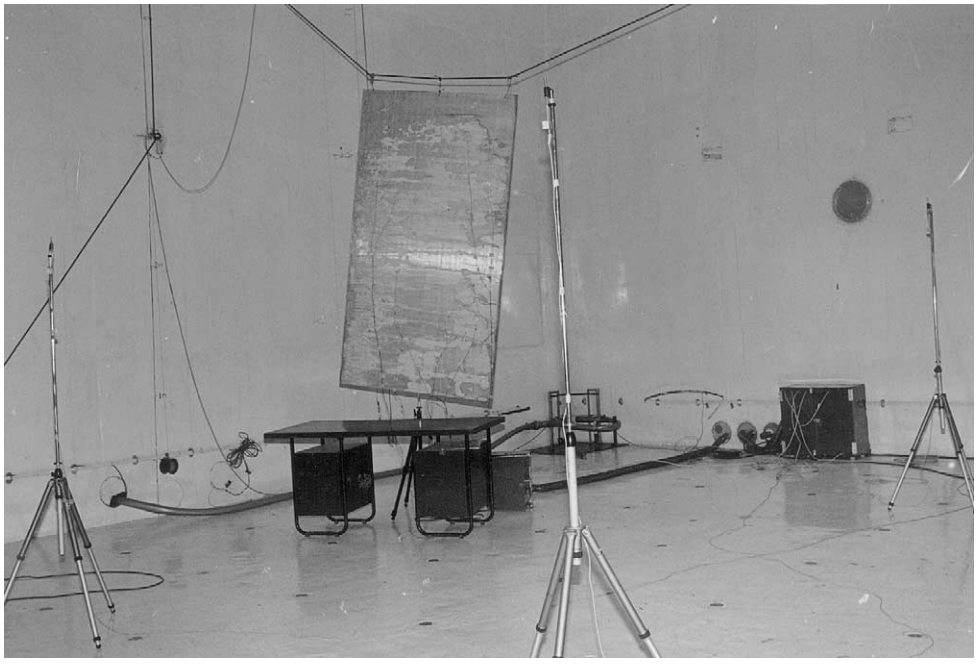

Figure 1. Test set-up for the acoustic test.

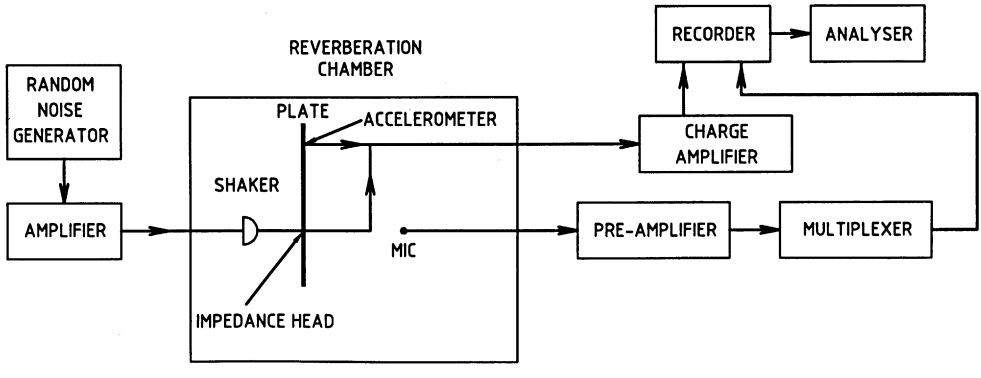

Figure 2. Schematic of vibration and sound measurement.

mean square values of the pressures are averaged. The microphones are fitted with suitable preamplifiers and 200 V polarization voltage is applied. The output of the microphone is recorded on a frequency-modulated (FM) tape recorder and analyzed off-line. Standard one-third octave band analyses of the vibration signals are carried out. Figure 2 gives a block diagram of the set-up for the measurement of sound pressure level. The shaker and the impedance head shown in the figure are for the measurement of dissipation loss factor.

Acceleration levels are measured using piezoelectric accelerometers at six randomly selected locations as shown in Figure 3. Since the modal density of the plate is very large, averaging over six locations gives a very accurate spatial average. It is to be noted that there are about 16 modes present in 400 Hz one-third octave band. This is the lowest frequency

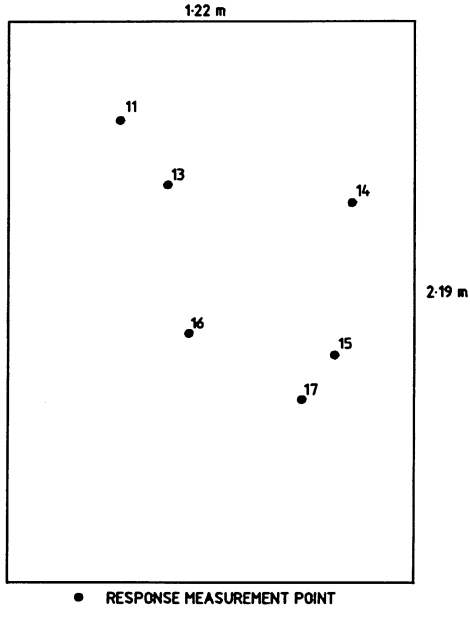

Figure 3. Accelerometer locations on the plate.

band where the results are presented. At any other frequency band, the number modes expected is still larger. One does not need even these many number of modes for obtaining the spatial average. The reason for presenting the results only from 400 Hz and above are discussed later. A schematic of the acceleration measurement is shown in Figure 3. The output of the accelerometer is conditioned using charge amplifier and the charge amplifier output is recorded on an FM recorder. The mass of each accelerometer is approximately 0·5 g. Average driving point impedance of the plate can be estimated using the equation

$$Z_p = 8(\rho D)^{0\cdot5}. \tag{3}$$

For the plate considered for the test, the average impedance is 844 Ns/m. The impedance due to accelerometer mass is 31·4 Ns/m at 10 000 Hz. Hence, the mass-loading effect of the accelerometer on the measured response is negligible. Acceleration sensitivity of these accelerometers is $\simeq$ 1·5 pC/g and the resonance frequency is 32 kHz with a useful frequency range of 5–8000 Hz ($\pm$ 5%). Hence, no corrections are applied in the measured acceleration levels. The results are given in terms of r.m.s. values in g in standard one-third octave bands from 400 to 10 000 Hz. The spatial average of the acceleration levels is given in Table 1 and Figure 4. The mean square values of acceleration levels are spatially averaged. The results below 400 Hz are not presented since the expressions for the radiation resistance are not accurate at low frequencies due to the effects of boundaries.

The expressions for radiation resistance available in the literature are for the simply supported boundaries [5–8]. At high frequencies, the boundary conditions do not affect the radiation resistance and the radiation resistance of a plate with any type of boundary is given by that of the plate with simply supported boundary. At low frequencies, the boundary conditions have significant effects on the radiation resistance. In the present case, the boundaries of the plate are free and hence the radiation resistance at low frequencies is expected to be very low. The frequency averaged radiation resistance of plates with free boundaries cannot be determined accurately. Since the main objective of the present work is

TABLE 1

Acceleration response of a plate

One-third octave band center frequency (Hz)	SPL (dB)	Acceleration response (g)	
		Theory	Experiment
400	113·0	0·21	0·20
500	113·4	0·24	0·23
630	112·5	0·23	0·31
800	111·8	0·23	0·29
1000	111·2	0·24	0·32
1250	112·4	0·39	0·39
1600	112·1	0·56	0·63
2000	110·9	0·81	0·85
2500	109·9	1·3	1·1
3150	109·6	1·4	1·1
4000	108·0	1·1	0·90
5000	107·5	0·90	0·83
6300	107·5	0·80	0·78
8000	107·2	0·70	0·75
10 000	107·2	0·63	0·56

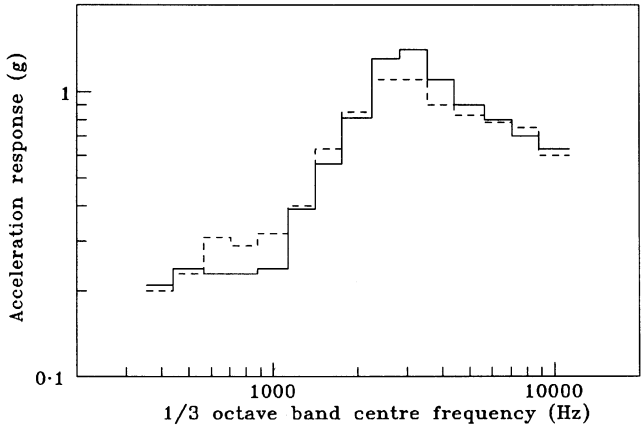

Figure 4. Response of a plate to reverberant acoustic field: ——, theory; and - - -, experiment.

to study the effect of the inclusion of non-resonant component in the response estimation and not the effect of boundaries, the responses are compared for frequencies where the radiation resistance converges to the radiation resistance of the simply supported plate. Otherwise, it will not be known whether the error is due to the boundary effect or the deficiency of the present investigation. If there are a few bending waves present in the structure, then the radiation resistance of the plate is approximately given by the radiation resistance of the simply supported plate. At 350 Hz, which is the lower bound of the 400 Hz one-third octave band, the wavelength is about 0·4 m and hence on average three bending waves are expected to be present in the structure. Hence, the results are compared only from 400 Hz one-third octave band onwards.

3. DISSIPATION LOSS FACTOR

There are some works on the dissipation loss factor of a plate reported in the literature. Cummins and Farrow [10] and Eaton [11] suggested that for frequencies between 80 and 2500 Hz, the dissipation loss factor values, denoted by η_d can be obtained from the expression

$$\eta_d = 1{\cdot}8/(f^{0{\cdot}87}). \tag{4}$$

For frequencies above 2500 Hz, the dissipation loss factor value can be considered to be 0·002. Still it is considered essential to determine the dissipation loss factor of the plate experimentally. This is because the response of the structure depends on many parameters including the dissipation loss factor. Unless all the parameters are obtained accurately, it will not be possible to study the effect of any of them on the estimated response.

The dissipation loss factor of the plate can be obtained experimentally using the energy method. The response level at several locations are measured for a known input power. From the equality of the input power and the dissipated power, the dissipation loss factor is obtained. Hence, for an input power of π_{in}, the dissipation loss factor is given by [12]

$$\eta_d = \pi_{in}/(\omega M \langle v^2 \rangle_x). \tag{5}$$

The plate has a mass M and $\langle v^2 \rangle_x$ is the spatial average of mean-square value of the velocity at circular frequency ω. The symbol $\langle\ \rangle_x$ represents spatial average. Clarkson and Pope [12] demonstrated this technique for plates and cylinders. In SEA, we require frequency averaged loss factors. In the frequency range where there is a large modal overlap, the frequency averaged loss factor is more meaningful. In the energy method, this can be achieved using frequency averaging or using random excitation with suitable bandwidths. Ranky and Clarkson [13] pointed out that in SEA-based calculations, energy average is the most appropriate which can be directly obtained when the energy method is used. The energy method is hence used to determine the loss factor.

The plate is hung in the reverberant chamber and excited at a point using a shaker. The excitation force is measured using an impedance head. The measurement set-up is shown in Figure 2. The input power is obtained using the relation [12]

$$\pi_{in} = f_p^2\, n(f)/(4M), \tag{6}$$

where f_p^2 is the mean-square value of the excitation force. The acceleration levels are measured at six randomly selected locations that are shown in Figure 2 and the spatial average of the mean square value of the velocity is calculated. The acceleration at the driving point is not considered for determining the average velocity of the structure [13]. Experiments are conducted with five driving point positions, that are shown in Figure 5, with one driving point excited at a time and the average taken over other locations. Substituting the expression for the power input in equation (5), the loss factor can be obtained using the relation

$$\eta_d = f_p^2\, n(f)/\{8\pi f M^2 \langle v^2 \rangle_x\}. \tag{7}$$

The loss factor thus obtained is given in Figure 6. The results are given only up to 5000 Hz since the excitation given at frequencies above 5000 Hz is very small and hence the loss factor determined can be in error. The experiment is conducted in air and hence the measured loss factor is the total loss factor, that is the sum of the dissipation loss factor and the radiation loss factor. Clarkson and Brown [14] have shown that if the total loss factor is used as the dissipation loss factor, the estimated response can be in large error. To obtain the dissipation loss factor, the radiation loss factor has to be substracted from the total loss

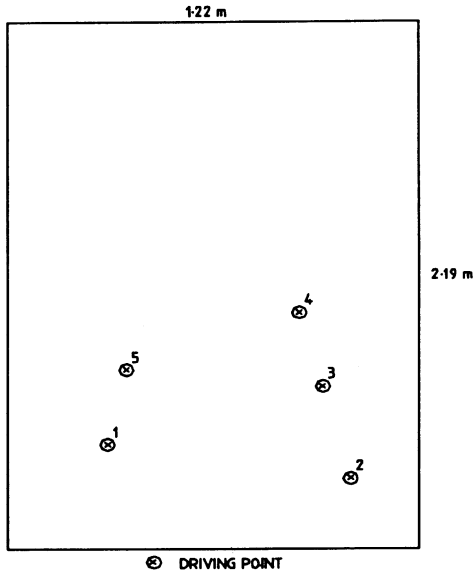

Figure 5. Driving point locations on the plate during the dissipation loss factor test.

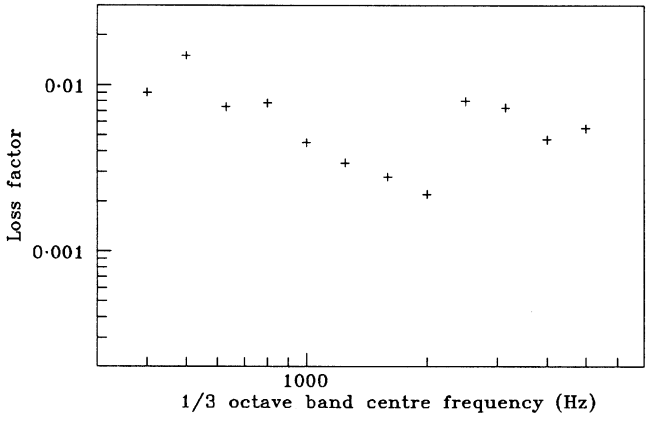

Figure 6. Total loss factor of the plate.

factor. The radiation loss factor is theoretically estimated using equations (19) and (11) that are to follow, and it is shown in Figure 7. The radiation resistance of this plate was obtained experimentally and it matched well with the theoretical estimates [9]. At low frequencies, since the radiation loss factor is very much dependent on the boundary conditions, the theoretical estimates of the radiation loss factor values are not accurate. Since the radiation loss factor itself is very low at low frequencies, the dissipation loss factor thus determined is not affected. The dissipation loss factor of the plate is shown in Figure 8.

The dissipation loss factor values obtained are of the same order as that reported by Cummins and Farrow [10] and Eaton [11]. Hence, equation (4) is used for the values of dissipation loss factor in the frequency range where the present experimental results are similar to those results. In frequency bands where there is a larger difference, the present results are used for the dissipation loss factor. Thus, the following values given in Table 2

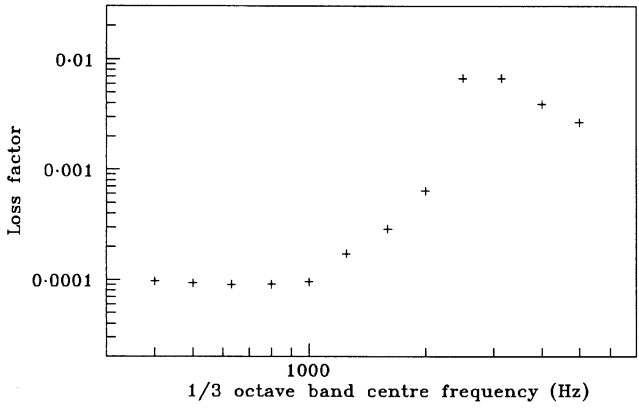

Figure 7. Estimated radiation loss factor of the plate.

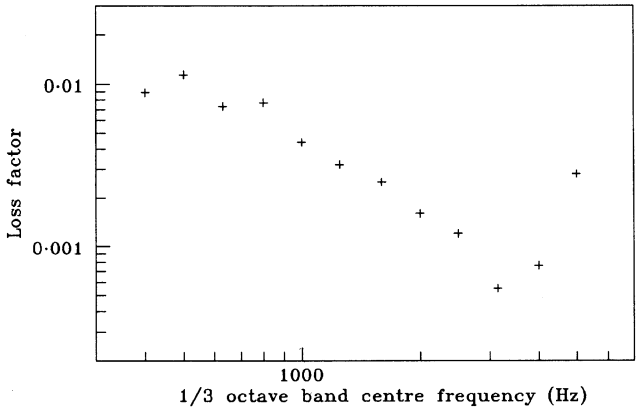

Figure 8. Dissipation loss factor of the plate.

TABLE 2

Dissipation loss factor of the plate

One-third octave band center frequency (Hz)	Dissipation loss factor
400	0·0099
500	0·0081
630	0·0066
800	0·0054
1000	0·0044
1250	0·0036
1600	0·0025
2000	0·0015
2500	0·0030
3150	0·0030
4000	0·0030
5000	0·0030

are used as the dissipation loss factors of the plate. It can be observed from Figure 8 that the measured dissipation loss factor near the critical frequency is very low. This is because the radiation loss factor is very large near the critical frequency and the dissipation loss factor is relatively low. Hence, the total loss factor is approximately the same as the radiation loss factor and the difference between them is not expected to be accurate. Hence, at those frequencies the dissipation loss factor values corresponding to the nearby frequency bands are used.

The radiation loss factor of a structure is very large near the critical frequency and hence the total loss factor increases to a large value at frequencies near the critical frequency. The results given in Figure 6 show that the total loss factor increases to a large value near 2500 Hz. The estimated critical frequency of the plate is 2512 Hz which is in close agreement with the experimental results. In the present experiment, it is assumed that the total power input is equal to the sum of the power dissipated and the power radiated. The power flowing from the acoustic field to the structure is negligible and hence not considered here. For example, the r.m.s. value of the acceleration level of the plate of 0·45 g at 2500 Hz and the sound pressure level in the room is 75 dB. The expected r.m.s. value of the acceleration response due to this sound field is about 0·042 g. The above data confirms that the power flowing from the acoustic field to the structure can be neglected in the present experiment. The data are presented for 2500 Hz since the radiated power is the maximum at frequencies near the critical frequency. Therefore, the loss factor will be slightly more than that obtained using equation (5). The sound power radiated is the sum of both the nearfield and the farfield radiated power. But the effect of neglecting the nearfield radiated power on the derived dissipation loss factor values is insignificant and hence in the present calculations, nearfield radiated power is not included. This is because above the critical frequency there is no sound radiation from the near field. And below the critical frequency the radiation loss factor is negligible compared to the total loss factor.

4. THEORETICAL ESTIMATION OF RESPONSE

When a plate is subjected to acoustic excitation its response is due to contributions from both resonant and non-resonant waves. It is shown that [3]

$$\langle v^2 \rangle_x = \langle v^2_{free} \rangle_x + \langle v^2_{forced} \rangle_x, \tag{8}$$

where v_{free} is the velocity due to the resonant response and v_{forced} is that due to the non-resonant response.

The resonant response of the plate can be estimated in SEA framework using a two-subsystem model where acoustic field is subsystem 1 and the structure is subsystem 2. Power balance of the subsystems form the following equation:

$$\begin{Bmatrix} \pi_1 \\ \pi_2 \end{Bmatrix} = \omega \begin{bmatrix} \eta_1 + \eta_{12} & -\eta_{21} \\ -\eta_{12} & \eta_2 + \eta_{21} \end{bmatrix} \begin{Bmatrix} E_1 \\ E_2 \end{Bmatrix}. \tag{9}$$

In equation (9), π_n, E_n and η_n are the power input, the mean energy and the dissipation loss factor respectively of nth subsystem. The coupling loss factor (CLF) for mth subsytem to the nth subsystem is denoted by η_{mn}. The power is supplied only to subsystem 1, that is the source room. Hence, by setting $\pi_2 = 0$, we get

$$E_2 = \{\eta_{12} E_1\}/\{\eta_2 + \eta_{21}\}. \tag{10}$$

The structure–acoustic coupling loss factor is determined from the radiation resistance of the plate. Hence,

$$\eta_{21} = R_{rad}/(\omega\rho A), \tag{11}$$

where R_{rad} is the radiation resistance of the plate. The acoustic–structure coupling loss factor is determined using the reciprocal law for coupling loss factors, as per which [1]

$$\eta_{12} = \eta_{21}\,(n_2/n_1). \tag{12}$$

where n_i is the modal density of subsystem i. The modal density of the acoustic space having volume V is given by

$$n(f) = 4\pi f^2 V/c^3. \tag{13}$$

The modal density of the plate can be estimated using equation (1).

The energy of the acoustic field is related to acoustic pressure in the source room by the equation

$$E_1 = (\langle p_1^2\rangle_x/\rho_a c^2)\, V_1, \tag{14}$$

where ρ_a is the density of the medium of the acoustic field and p is the acoustic pressure. Substituting equations (11–14) in equation (10), the energy of the plate can be estimated. The energy of the plate is related to the velocity of the plate by the equation

$$\langle v_{free}^2\rangle_x = E_2/\rho A. \tag{15}$$

The velocity determined above is that due to the resonant waves.

Velocity of the non-resonant waves due to a diffuse acoustic field can be determined using the equation [9]

$$\langle v_{forced}^2\rangle_x = (\langle p^2\rangle_x/4\rho_a^2 c^2)\,\tau_r, \tag{16}$$

where ρ_a is the density of the acoustic medium. In the above equation, τ_r represents the random incidence sound power transmission coefficient of the structure. The random incidence sound power transmission coefficient is defined as the ratio of the expected sound power transmitted to the expected incident power. It is then give by [3]

$$\tau_r = 2\int_0^{\pi/2} \tau \sin\theta\cos\theta\,\mathrm{d}\theta, \tag{17}$$

where τ is the sound power transmission coefficient of the structure. In practical situations, a field incidence transmission coefficient is used in which the angle of incidence is restricted to the range 0–78°. For panels having stiffness, the sound power transmission coefficient can be obtained using the equation [15]

$$\tau^{-1} = \{1 + \eta_d a\cos\theta\sin^4\theta\,(f/f_c)^2\}^2 + \{a\cos\theta\,(1 - (f/f_c)^2\sin^4\theta)\}^2. \tag{18}$$

The plate has a critical frequency of f_c and the acoustic field strikes the panel with an angle of incidence θ. The parameter a is equal to $(\rho\omega/2\rho_a c)$.

The total response of the plate can now be obtained using equation (8). The differences between the approach used here and elsewhere are that in the present method the non-resonant response component is included [9] and the modified expressions for the radiation resistance are used [8]. Inclusion of the non-resonant part in the response calculations can be done even in the SEA modelling itself as proposed by Renji *et al.* [9].

The expressions for the radiation resistance of a simply supported plate whose dimensions are a, b are as follows.

For $f < f_c$ and ka, $kb > 2\pi$:

$$R_{rad} = A\rho_a c \{(\lambda_c \lambda_a / A)\ 2\ (f/f_c)\, g_1 + (p\lambda_c/A)\, g_2\}/2,$$

where

$$g_1 = (4/\pi^4)\ \{(1 - 2\psi^2)/[\psi\ (1 - \psi^2)^{1/2}]\} \quad \text{for } f/f_c < 0{\cdot}5,$$

$$g_1 = 0 \quad \text{for } f/f_c \geqslant 0{\cdot}5,$$

$$g_2 = (1/4\pi^2)\ \{(1 - \psi^2)\, ln\,[(1 + \psi)/(1 - \psi)] + 2\psi\}\ \{1/(1 - \psi^2)^{3/2}\},$$

$$\psi = (f/f_c)^{1/2}.$$

For $f < f_c$ and ka, $kb < 2\pi$:

$$R_{rad} = \mathrm{A}\rho_a c\ (4/\pi^4)(p\lambda_c/A)\ (f/f_c)^{1/2}/2.$$

For $f = f_c$:

$$R_{rad} = \mathrm{A}\rho_a c\ \{(a/\lambda_c)^{1/2} + (b/\lambda_c)^{1/2}\}/2.$$

For $f > f_c$:

$$R_{rad} = \mathrm{A}\rho_a c\ \{1 - (f_c/f)\}^{-1/2}. \tag{19}$$

In equation (19), p is the perimeter of the plate and k is the wavenumber. The wavelength of sound in air is denoted by λ_a and the wavelength at critical frequency is denoted by λ_c. The difference between the presently used expressions for the radiation resistance and the existing expressions is the presence of factor 2 for frequencies up to the critical frequency of the plate.

In this case, the radiating area of the plate is twice the area of the plate. The plate used in this study has free boundaries. The experimental results are obtained for a free–free plate, whereas the theoretical estimates are made for a simply supported plate. In the low-frequency range, the boundary conditions affect the radiation resistance significantly. Effect of boundary conditions is not significant if the plate carries a few bending waves and in such a frequency range the radiation resistance is given by the radiation resistance of the simply supported plate. In the present case at 400 Hz, there are three bending waves present in the plate. Since the plate is unbaffled, a factor of 0·5 up to a frequency of $f_c/2$ is applied to take into account the effect of neighboring structure on the radiation resistance [8]. In addition to the above effects, short-circuiting effects due to the absence of the baffle are also considered and the effects are included using the following relations [16]:

$$R_{rad} = F_p\ \{F_c R_{rad,c} + F_e R_{rad,e}\}, \tag{20}$$

where $R_{rad,c}$ and $R_{rad,e}$ are the radiation resistance of corner and edge modes, respectively, F_p is the correction factor for the flow around the plate and F_c and F_e are the correction factors for the flow near the edges for the corner as well as the edge modes respectively. These correction factors are given below [16].

$$F_c = 13\ (f/f_c)/\{1 + 13\ (f/f_c)\},$$

$$F_e = 49\ (f/f_c)/\{1 + 49\ (f/f_c)\},$$

$$F_p = 53 f^4 A^2/c^4/\{1 + 53 f^4 A^2/c^4\}. \tag{21}$$

The correction factors F_c and F_e are significant only at low frequencies and F_p is important only when the acoustic wavelength is larger than the plate dimensions. In the present case, the correction factor F_p is not used, as the effect due to this is very much insignificant even at

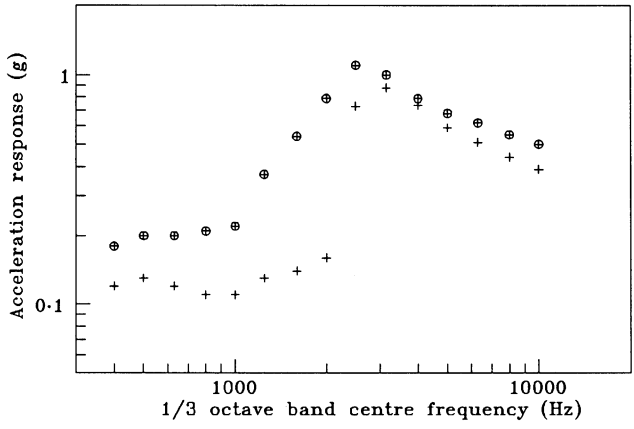

Figure 9. Comparison of resonant and non-resonant responses: ⊕, resonant; and +, non-resonant.

400 Hz. At 400 Hz, the correction factor F_p is equal to 0·999. It is to be noted that the radiation resistance of the same plate was obtained experimentally [8] and the results match very well with the theoretical estimates made using the expressions and the factors discussed above.

The estimated total acceleration response is given in Table 1 and Figure 4. The dissipation loss factor is experimentally obtained only up to 5000 Hz. Hence, for frequencies above 5000 Hz, the dissipation loss factor value at 5000 Hz is used. The response levels are presented as r.m.s. values in g in the standard one-third octave bands from 400 to 10 000 Hz. The responses below 400 Hz are not presented since the radiation resistance values in these frequency bands are not estimated accurately as discussed previously.

5. DISCUSSION OF RESULTS

The measured acceleration levels of the plate are compared with the theoretical estimates in Table 1 and Figure 4. They show a reasonably good agreement. The estimated response levels are larger compared to the measured results at frequencies near the critical frequency. This is because, near the critical frequency, the theoretical expressions for the resonant as well as the non-resonant responses predict higher values which do not occur in practice.

The significance of the non-resonant response can be seen from Figure 9 where both resonant and non-resonant responses are compared. It can be seen that the non-resonant response is as significant as resonant response especially at frequencies near and above the critical frequency. From the above results, it follows that if the non-resonant part is not considered the response could be largely underestimated especially at frequencies near and above the critical frequency.

In all the above results, the non-resonant response is estimated using the thin plate model, that is the sound power transmission coefficient is represented by equation (18). A comparison of the non-resonant response of the plate estimated using the limp panel model and that using the thin plate model is given in Figure 10. For a limp panel, the stiffness is negligible and the sound transmission characteristics is represented by [15]

$$\tau^{-1} = 1 + \{\rho\omega/(2\rho_a c)\}^2 \cos^2\theta. \tag{22}$$

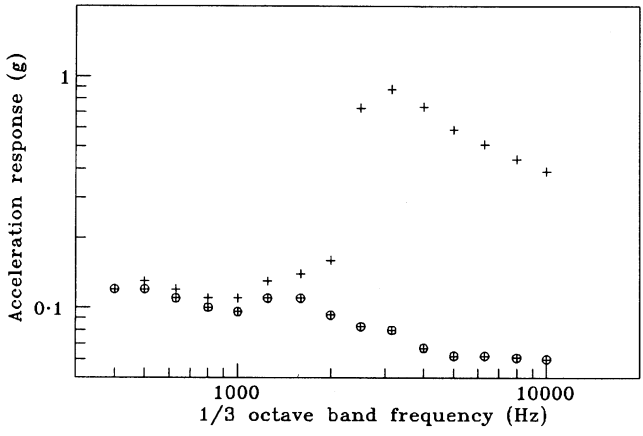

Figure 10. Non-resonant response of a plate for different models: ⊕, limp panel; and +, thin plate.

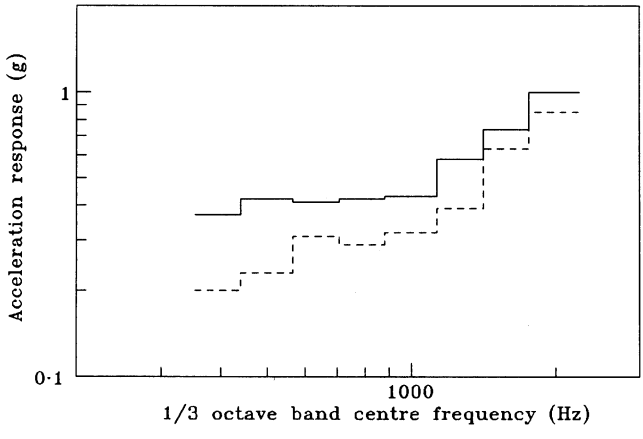

Figure 11. Comparison of the measured response of a plate with the response estimated using the existing expressions for radiation resistance: ——, theory; and - - -, experiment.

It can be seen that if limp panel model is used to represent the sound transmission behavior, the response levels are estimated to be very small at frequencies near and above the critical frequency. This might be the reason that the non-resonant response was considered to be insignificant. It is also important to mention that the non-resonant response is lower for massive structures like buildings. Perhaps this could also be the reason for the belief that the non-resonant response of the structure is not that significant. The present results clearly indicate the need for incorporating the non-resonant part in the response estimation.

It is of interest to compare the measured results with the response estimated using the existing expression for the radiation resistance [5–7]. Since the existing expression overestimates the radiation resistance, it is expected that the response levels are also overestimated though they are not directly proportional. Both the results are shown in Figure 11. Since the differences in the expressions for the radiation resistance exist only up to the critical frequency, the results are compared only up to the one-third octave band centered at 2000 Hz. The results show that the response levels are overestimated by using the existing expression for the radiation resistance. It is to be noted that the response levels do not depend only on the radiation resistance and hence comparing the response will not

be as effective as comparing the radiation resistance. Even then the results show significant effects.

The response predicted by SEA is the average over an ensemble of systems. But the present experimental results are for a single system. Assuming ergodicity for the frequency response functions for the ensemble of structures, one can use frequency averaging in place of ensemble averaging. Normally, frequency averaging is used and the same is followed in the present case.

So far in our discussions, only the mean values of the response levels are referred. It is also important to estimate the variance. Taking into account the uncertainties in the energy of the directly excited subsystem, the randomness of the structural properties and variations in the observation points, and the variance in the response of the indirectly excited subsystem in the frequency band $\Delta\omega$ can be determined using the equation [1]

$$\frac{\sigma_{a^2}^2}{m_{a^2}^2} = \left\{ n_1 n_2 \frac{\pi}{2} \Delta\omega (\Delta_1 + \Delta_2) \right\}^{-1} \left\{ \frac{\langle \psi_1^4 \rangle_x}{\langle \psi_1^2 \rangle_x^2} \right\} \left\{ \frac{\langle \psi_1^4 \rangle_x \langle \psi_2^4 \rangle_x}{\langle \psi_1^2 \rangle_x^2 \langle \psi_2^2 \rangle_x^2} \right\} \left\{ \frac{\langle \psi_2^4 \rangle_x}{\langle \psi_2^2 \rangle_x^2} \right\}, \tag{23}$$

where ψ is the mode shape and Δ_i is the half-power bandwidth of subsystem i and subsystem 1 is directly excited. Let σ_{a^2} be the variance and m_{a^2} be the mean value of the mean-square value of the acceleration response. In the present problem, it is seen that the variance is very small. For example, in 1000 Hz, one-third octave band $\sigma_{a^2}^2/m_{a^2}^2 = 0{\cdot}0006$. This is because of the presence of large number of modes in the acoustic field.

The variance due to observation points on the panel can be estimated using the results of Stearn [17] as per which

$$\sigma_{a^2}^2/m_{a^2}^2 = 2{\cdot}121/(N)^{1/2}, \tag{24}$$

where N is the number of modes. As per the analysis of Stearn [17], the mean-square values of the acceleration responses follow normal distribution is there are more than 10 modes present in the given frequency band. In the present case, there are 16 models in 400 Hz octave band and at higher frequencies there are even more number of modes.

It is now possible to estimate the confidence intervals for a given confidence coefficient with the help of the estimated mean and variance and known probability density function for the distribution. It is more appropriate to estimate the "exceedance" type of confidence interval. That is to find the response level such that any realized value will be less than that with a specific probability, called confidence coefficient. The response levels with 99% of the realizations have the response levels lower than this value, which are estimated and shown in Figure 12. The acceleration levels are measured at six locations and they are also given in the same figure. One can see a reasonably good prediction.

It is worth studying the confidence intervals estimated by neglecting the non-resonant response. The results are shown in Figure 13. The non-resonant response is more significant near and above the critical frequency. It can be seen that at large number of points the measured acceleration levels exceed the predicted levels showing the importance of including the non-resonant part in the response prediction.

In the above calculations, σ/m of the resonant response is taken even for the non-resonant response. This is yet to be established. It is important to note that the non-resonant response is more significant at higher frequencies and at higher frequencies the variance is very negligible. For example, at 10 000 Hz the mean-square value of the resonant response is $0{\cdot}25\ g^2$ and the non-resonant response is $0{\cdot}15\ g^2$. The variance of the resonant response is $0{\cdot}027\ g^2$. The variance of the non-resonant response is $0{\cdot}017\ g^2$. Hence, some error in the

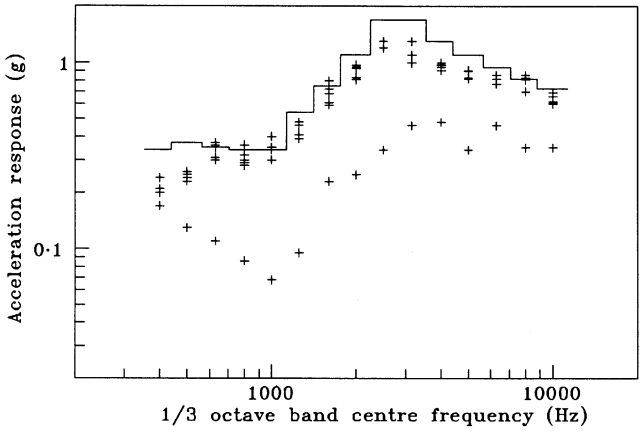

Figure 12. Comparison of the estimated response levels for a confidence of 99% with the measured realizations: ——, predicted; and +, measured realizations.

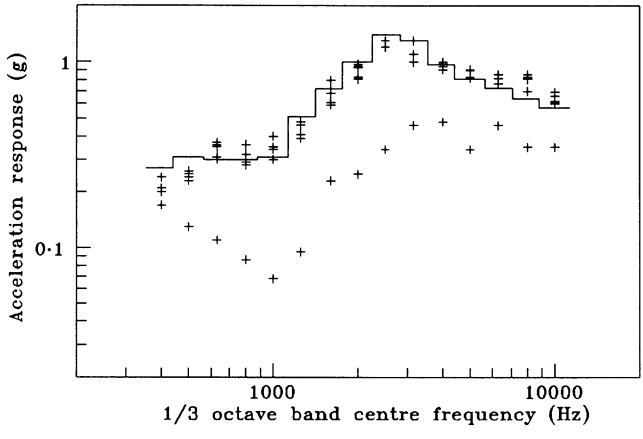

Figure 13. Effect of the non-resonant component on the estimated response levels for a confidence of 99%: ——, predicted neglecting the non-resonant part; and +, measured realizations.

estimation of the variance of the non-resonant response will not make a significant difference in the estimated confidence levels.

6. CONCLUSIONS

The acceleration levels of a typical plate under acoustic excitation are obtained experimentally and compared with the theoretical estimates. The theoretically determined response levels match reasonably well with the experimental results. The theoretical estimates are made using the modified expressions for the radiation resistance and the non-resonant response component is included in the response estimation. The dissipation loss factor of the plate is obtained from the experiments. It is seen that the non-resonant response is as significant as the resonant response at frequencies near and above the critical frequency. If the non-resonant part is not considered, then the estimated response levels are significantly lower than the measured results. The measured vibration levels are above the

estimated response levels for 99% confidence coefficient if the non-resonant response is not taken into account. It is thus essential that the non-resonant response component be included in the response estimation. The measured results are significantly lower compared to the predictions made using the existing expressions for the radiation resistance but match reasonably well if they are estimated using the modified expression for the radiation resistance.

ACKNOWLEDGMENTS

The authors wish to thank Mr K. N. ArunKumar, Mr K. R. Chandrasekhar and Ms D. Padmini of Acoustic Test Facility, National Aerospace Laboratories, Bangalore, India, for their valuable help in conducting the experiments.

REFERENCES

1. R. H. LYON 1975 *Statistical Energy Analysis of Dynamical Systems*: *Theory and Applications*. Cambridge, MA: MIT Press.
2. R. H. LYON 1963 *Journal of the Acoustical Society of America* **35**, 1791–1797. Noise reduction of rectangular enclosures with one flexible wall.
3. M. HECKL 1981 *Journal of Sound and Vibration* **77**, 165–189. The tenth Sir Richard Fairey Memorial Lecture: sound transmission in buildings.
4. M. P. NORTON 1989 *Fundamentals of Noise and Vibration Analysis for Engineers*. England: Cambridge University Press.
5. G. MAIDANIK 1962 *Journal of the Acoustical Society of America* **34**, 809–826. Response of ribbed panels to reverberant acoustic fields.
6. M. J. CROCKER and A. J. PRICE 1969 *Journal of Sound and Vibration* **9**, 469–486. Sound transmission using statistical energy analysis.
7. G. MAIDANIK 1975 *Journal of the Acoustical Society of America* **57**, 1552 (Erratom: Response of ribbed panels to reverberant acoustic fields).
8. K. RENJI, P. S. NAIR and S. NARAYANAN 1998 *Journal of Sound and Vibration* **212**, 583–598. On acoustic radiation resistance of plates.
9. K. RENJI, P. S. NAIR and S. NARAYANAN 2001 *Journal of Sound and Vibration* **241**, 253–270. Non-resonant response using statistical energy analysis.
10. R. J. CUMMINS and I. R. FARROW 1981 *ESA CR*(*P*) 1609, Vol. 1. Study of the evolution of structural acoustic design guides.
11. D. C. G. EATON 1987 *ESA PSS*-03-1201, Issue 1. Structural acoustic design manual.
12. B. L. CLARKSON and R. J. POPE 1981 *Journal of Sound and Vibration* **77**, 535–549. Experimental determination of modal densities and loss factors of flat plates and cylinders.
13. M. F. RANKY and B. L. CLARKSON 1983 *Journal of Sound and Vibration* **89**, 309–323. Frequency average loss factors of plates and shells.
14. B. L. CLARKSON and K. T. BROWN 1985 *Transactions of the American Society of Mechanical Engineers*, *Journal of Vibration*, *Acoustics*, *Stress and Reliability in Design* **107**, 357–360. Acoustic radiation damping.
15. D. D. REYNOLDS 1981 *Engineering Principles of Acoustics*, *Noise and Vibration*. Boston, MA: Allyn & Bacon.
16. C. H. OPPENHEIMER and S. DUBOWSKY 1997 *Journal of Sound and Vibration* **199**, 473–489. A radiation efficiency for unbaffled plates with experimental validation.
17. S. M. STEARN 1970 *Journal of Sound and Vibration* **12**, 85–97. Spatial variation of stress, strain and acceleration in structures subjected to broad frequency band excitation.

APPENDIX A: LIST OF SYMBOLS

Symbols not listed here are used only at specific places and are explained wherever they occur. Since the process considered is stationary random, the dynamic variables discussed

are the long time averaged quantities and in such cases, the notation for the averaging is dropped. For example, $\langle a^2 \rangle_t$ is written as a^2.

A	area of a plate
a	acceleration response of a structure
a, b	dimensions of a panel
c	speed of sound in air
D	flexural rigidity
E_i	mean energy of subsystem i
F_c	correction factor for flow around the edge, for a corner mode
F_e	correction factor for flow around the edge, for an edge mode
F_p	correction factor for the flow around the plate
f	frequency, in Hz
f_c	critical frequency, in Hz
f_p	applied force
k	wavenumber
M	mass of a structure
m_x	mean of the random variable x
N	number of modes of a subsystem in a frequency band
$n(f)$	number of modes per Hz
p	acoustic pressure
p_i	acoustic pressure in subsystem i
R_{rad}	radiation resistance of a structure
$R_{rad,c}$	radiation resistance of a corner mode
$R_{rad,e}$	radiation resistance of an edge mode
V	volume
V_i	volume of subsystem i
v	velocity of a structure
v_{forced}	velocity of the forced wave
v_{free}	velocity of the free wave
Z_p	driving point impedance of a structure
Δ_i	half-power bandwidth of oscillator/subsystem i
$\Delta\omega$	frequency band, in rad/s
η_d	dissipation loss factor
η_i	dissipation loss factor of oscillator/subsystem i
η_{ij}	coupling loss factor for subsystem i to j
λ_a	wavelength in the acoustic field
λ_c	wavelength at the critical frequency
π_{in}	input power
π_i	power input to subsystem i
ω	circular frequency, in rad/s
ω_c	critical frequency, in rad/s
ρ	mass per unit area
ρ_a	density of the medium of the acoustic field
σ_x	standard deviation of the random variable x
θ	angle of incidence
τ	sound power transmission coefficient of a structure
τ_r	random incidence sound power transmission coefficient of a structure
θ	angle of incidence
$\langle\,\rangle_x$	average over the domain x
$\langle\,\rangle$	average over the time domain